Effect of Iron Oxide Nanoparticles on the Morphological Properties of Isotactic Polypropylene

Yousef Ahmad Mubarak, Fatima O. Abbadi, Ahmed H. Tobgy

Department of Chemical Engineering, Faculty of Engineering and Technology, University of Jordan, Amman 11942, Jordan

Received 19 June 2009; accepted 31 August 2009
DOI 10.1002/app.31374
Published online 4 November 2009 in Wiley InterScience (www.interscience.wiley.com).

ABSTRACT: Isotactic polypropylene (iPP) and iron oxide (Fe_3O_4) nanocomposites were mixed by masterbatch blending technique in a single screw extruder machine. The concentrations of Fe_3O_4 in the iPP/Fe_3O_4 nanocomposites were 0.5, 1, 2, and 5% by weight. The influence of Fe_3O_4 nanoparticles on the effectiveness of nucleation, morphology, mode of crystallization, and crystallinity of iPP were studied by differential scanning calorimetry (DSC) and polarized light microscopy (PLM). The introduction of Fe_3O_4 nanoparticles in the iPP matrix inhibited the formation of β crystals, and caused a shift in the melting point to higher values. The magnitude of the shift was up to 20–21°C which indicates that using the masterbatch technique leads to an enhancement of the dispersion process of the Fe_3O_4 nanoparticle and the formation of less agglomerates in the iPP/Fe_3O_4 nanocomposites. The percentage crystallinity, X_c, increased at the low cooling rates of 1 and 2°C/min. At higher cooling rates of 5, 10, and 20°C/min, the masterbatch technique produced nanocomposites of X_c with nonuniform trends. The overall crystallization rate enhancement for the iPP/Fe_3O_4 nanocomposites is attributed to the presence of Fe_3O_4 nanoparticles as a nucleating agent which have no significant effect on the growth rate of iPP crystals. J Appl Polym Sci 115: 3423–3433, 2010

Key words: polypropylene; iron oxide nanoparticles; nanocomposites

INTRODUCTION

Polypropylene (PP) is a semicrystalline polymer which is widely used in industrial and commercial applications due to its properties of low cost, density, and ease of processing.[1,2] PP exhibits three common crystalline forms; monoclinic α, hexagonal or trigonal β and triclinic γ, distinguished by the arrangement of the chains.[2–4] The most common crystalline form of pure PP is the α-form which is the most stable with a density of 0.936 g/cm^3 and a melting point of 165°C. The β-form of PP was first observed by Keith et al. in 1959.[4] It has a trigonal cell structure with more disorder than the α-form. A high amount of β-form can be produced under special crystallization conditions, while the temperature gradient is applied or when selective β-nucleating agents are presented.[3,5] The growth rate of β-form exceeds the α-form (70% higher),[4] while the melting point is much lower, in the intervals of 145–150°C.[3] The third crystalline form of PP is the γ-form or triclinic, which is observed only under specific conditions, such as low molecular weight, crystallization at elevated temperature.[2]

Correspondence to: Y. A. Mubarak (ymubarak@ju.edu.jo).

Journal of Applied Polymer Science, Vol. 115, 3423–3433 (2010)

Over the years, researchers have sought to further expand the utility of PP, through the addition of nanoadditives, thereby creating a nanocomposite material with a careful selection of the matrix and the nanoadditives for obtaining the optimal property enhancement. Frequently, the size, geometry, and mechanical stiffness of nanoadditives play a critical role in final nanocomposite properties.[6] Polymer nanocomposites have attracted considerable interests owing to their outstanding mechanical properties, like elastic stiffness and strength, with only a small amount of the nanoadditives.[7] In addition, large influences on crystallization process, degree of crystallinity, and nucleation have been reported.[8] This is caused by the large surface area to volume ratio of nanoadditives when compared to the micro- and macro-additives.[7]

There are several experimental methods to produce polymer nanocomposites such as: solution blending, melt blending, *in situ* polymerization, chemical modification of nanoparticles, and the use of surfactants.[9] The melt-blending approach can be an effective method for industrial application and is much more commercially attractive than the other methods, as solution blending, chemical modifications and *in situ* polymerization are less versatile and more environmentally contentious.[6,10] However, homogeneous dispersion of nanoparticles in a polymer matrix using direct melt blending can be

scarcely obtained.[9] Masterbatch melt blending technique is reported to obtain better dispersion and properties than the direct melt blending. In Masterbatch melt blending, concentrates are prepared and let down with the bulk of polymer.[11]

The most common nanoadditives that were used in PP were clay, talc, silica, calcium carbonate, and metal oxides. Polymer/metal oxide nanocomposites provide flexibility in designing advanced materials. The incorporating of nanoscale metal oxide particles improves the mechanical and chemical properties of polymers.[12] It was discovered that nanoscale iron oxides [(II) and iron(III) oxides as well as mixed iron(II) and iron(III) oxides, for example Fe_2O_3 or Fe_3O_4] result in the formation of a high content of β-crystalline PP on cooling of a PP melt comprising these iron oxides. An increased content of the β-crystal modification in therefore has a favorable effect on certain service properties of the PP in some applications such as the production of films, moldings, in particular pipes and tubes, fibers and other extrusions.[13]

Thus, the objective of this work described here is to study the effect of iron oxide (Fe_3O_4) nanoparticles on the nucleation, mode of crystallization, morphology and crystallinity of isotactic polypropylene (iPP). The preparation method used in this work is melt and masterbatch melt blending using a single screw extruder.

EXPERIMENTAL

Materials

Isotactic polypropylene homopolymer grade (587P), provided by Sabic Co. KSA, was used as the matrix material in this study. iPP has a melt flow index (MFI) of 25 g/10 min and a density of 905 kg/m^3. Fe_3O_4 nanoparticles, provided by Arry International Group Limited-Germany, were used as nanofiller for iPP. Fe_3O_4 with the black color and spherical morphology has an average particle size of 20 nm, a purity of >99.5%, a surface area of >60 m^2/g and a bulk density of 0.84 g/cm^3.

Preparation of iPP/Fe_3O_4 nanocomposites

The blending was carried out in a single screw extruder (Axon ab10 Mini Extruder-Sweden) with a 10 mm screw diameter, 20xD L/D-ratio and four temperature regulators with thermocouples at temperatures of 170, 185, 195, and 210°C from the feed zone to the exit die. The Hopper was fed by employing direct addition of iPP granules and Fe_3O_4 nanopowders in 10 wt % concentration, which were then fed into the barrel for melting. On the exit from the die, the polymer strand passed through a water bath at room temperature and then chopped to small pieces using Axon ab Pelletizer machine by a steel blade. To ensure more homogenous blending and dispersion of Fe_3O_4 nanoparticles in the iPP matrix, the chopped extruded pieces were cycled through the extruder twice. Extruder's temperature zones were kept in the range from 170 to 210°C to avoid thermal degradation during the cycling, and then checked by differential scanning calorimetry (DSC) in which melt scans were identical. The 10 wt % Fe_3O_4 concentration of iPP/Fe_3O_4 nanocomposite that was prepared using direct melt blending technique was used as the masterbatch. Nanocomposites with Fe_3O_4 concentrations of 0.5, 1, 2, and 5 wt % were prepared from the masterbatch sample using dilution method. The extruded strands produced where recycled to the hopper and extruded once more.

Polarized light microscopy (PLM)

A polarized light microscopy (PLM) (ML9430-Meiji Techno-Japan) equipped with a (Mettler FB82-USA) hot stage and a Sony digital camera was used to study the crystallization morphology and spherulite growth rate of the virgin iPP and the prepared composites. The PP sample that was sandwiched between two microscope cover glasses was first melted at 200°C, pressed into thin film, and then maintained at 200°C for 3 min to achieve thermal equilibrium.

For the isothermal crystallization, the sandwiched sample was cooled to the required crystallization temperature (135, 140, 145, and 150°C) at a rate of 40°C/min. The temperature was maintained during the period of time required to complete the crystallization process. For the nonisothermal crystallization, the sample was cooled to the room temperature at the required cooling rate (1, 2, 5, 10, and 20°C/min). A Sony digital camera fixed on top of the microscope tube and connected to the PC by a TV card and a video recorder software were used to record the crystallization process and hence the growth of the spherulites. Several samples were tested twice or three times to ascertain the reproductility of the results. Images were analyzed by measuring the spherulite radius as a function of time.

Differential scanning calorimetry (DSC)

Nonisothermal crystallization was carried out on a Mettler Toledo DSC823-Germany. Pure Indium was used as a reference material to calibrate both the temperature scale and the melting enthalpy before the samples were tested. A sample of (0.5 ± 0.2) mg was first heated from 25 to 200°C with the presence of Nitrogen atmosphere and kept at this temperature for 3 min to eliminate any thermal history; the

sample was then cooled at the required rate (1, 2, 5, 10, or 20°C/min) to 50°C. A heat scan at 10°C/min was then carried out from 50 to 200°C to obtain the final sample enthalpy of fusion. Several samples were tested twice or three times to ascertain the reproducibility of the results.

The enthalpy of fusion, ΔH_{sample} is calculated by integrating the area under the melting peak and then dividing the result by the weight of the polymer sample. In addition the % crystallinity is calculated using the following relation.[5,14–16]

$$\% \text{ crystallinity} = \frac{\Delta H_{sample}}{\Delta H_{ref}} \times 100\% \quad (1)$$

where ΔH_{sample} is the enthalpy of fusion for the sample under study (J/g) and ΔH_{ref} is the enthalpy of fusion for a 100% crystallinity PP sample = 209 (J/g).

RESULTS AND DISCUSSION

Effect of Fe_3O_4 nanoparticles on the morphological properties of iPP

Crystalline morphologies were studied by PLM during isothermal crystallization at temperatures of 135, 140, 145, and 150°C and nonisothermal crystallization at cooling rates of 1, 2, 5, 10, and 20°C/min.

Only the monoclinic α phase was present in all isothermal and nonisothermal crystallized samples while no hexagonal β phase was observed by PLM.

The results display the common spherulites with sharp and clear birefringence. The growth of the spherulites, impeded by neighboring spherulitic structure, results in polygonal shapes confirmed by straight lines as shown in Figure 1(a), or hyperbolas boundaries as shown in Figure 1(b). Usually, when the spherulites are nucleated simultaneously, straight lines boundaries are observed. On the other hand hyperbolas boundaries are observed when spherulites nucleate at different times, due to the linear increase of the spherulite radius with time, during growth.[17]

The effect of crystallization temperature on the iPP morphology with and without Fe_3O_4 nanoparticles can be observed in the micrographs in Figures (2 and 3).

The micrographs show a decrease in the spherulite size upon decreasing the crystallization temperature while the number of spherulites per unit area increases. The enhancement of nucleation by the addition of Fe_3O_4 nanoparticles can be noticed from the results at all crystallization temperatures. As the number of nuclei increases the spherulites in the composite will impinge at an early time in a limited space, thus could end up in a smaller spherulite size and an increase in the number of spherulites compared with the pure iPP. Additionally, at lower crystallization temperature, one can observe how the iPP spherulites were not well defined and their sizes were very small. This indicates the nucleation effect of the nano Fe_3O_4 and the increase of supercooling which increases the nuclei [Fig. 4 (a,b)].

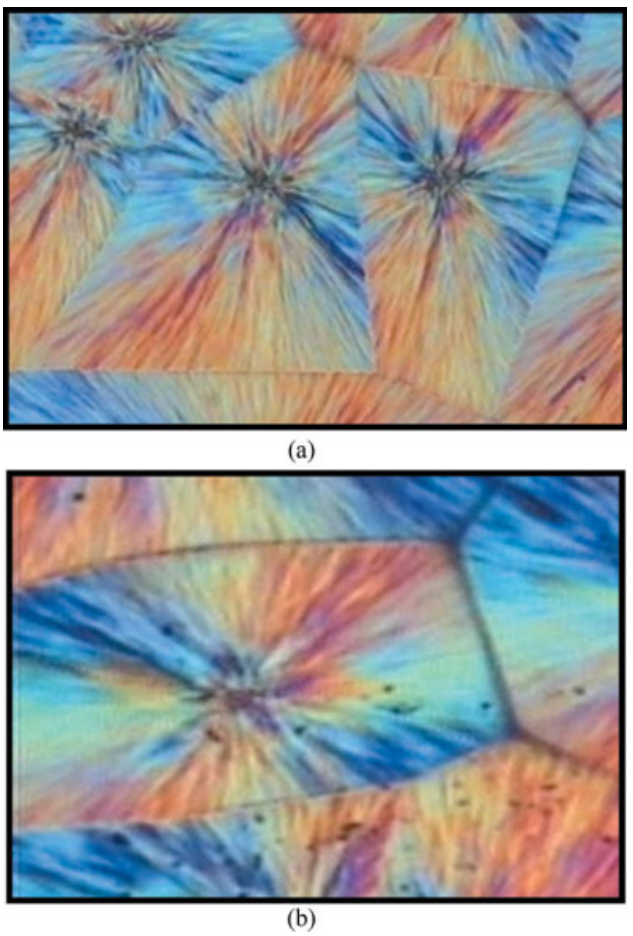

Figure 1 (a) Linear boundary lines between α–spherulites; (b) hyperbolas boundary between α–spherulites. [Color figure can be viewed in the online issue, which is available at www.interscience.wiley.com.]

Effect of Fe_3O_4 nanoparticles on the iPP spherulites growth rate

Spherulites growth rates were measured by PLM. The radius of the growing crystals was monitored during solidification by taking photomicrographs at appropriate intervals of time. Figure 5(a,b) shows a typical example for the relationship of spherulite radius (r) versus time (t) for pure iPP and iPP/Fe_3O_4 nanocomposites measured isothermally at temperatures of 135, 140, 145, and 150°C. Spherulites growth rates are reported at these high temperatures only because it was so difficult to observe the growth rates under the microscope at lower crystallization

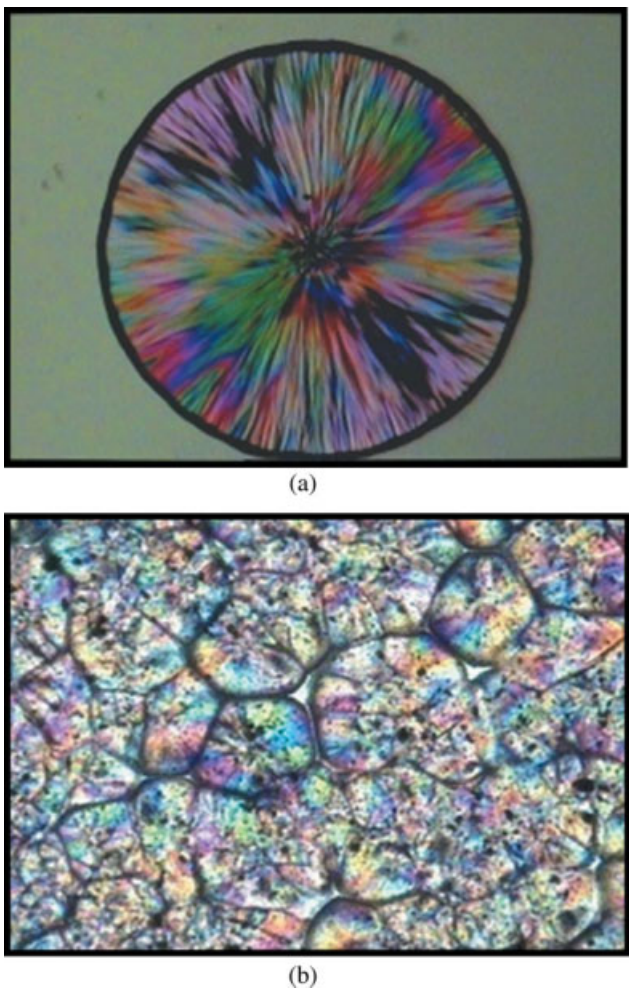

Figure 2 (a) iPP (b) 2% iPP/Fe_3O_4 nanocomposite samples crystallized at temperature 150°C. [Color figure can be viewed in the online issue, which is available at www.interscience.wiley.com.]

temperatures, especially for the nanocomposites with 1 and 2 wt % of Fe_3O_4 nanoparticles.

It can be seen that the radius of the iPP/Fe_3O_4 spherulites increases linearly with time until impingement occurs, similar to that of pure iPP. Moreover, the slope of the curve generally decreases with the increase of crystallization temperature due to the decrease in supercooling.

Spherulite growth rate (G) is generally measured at isothermal conditions, by monitoring the variation of the spherulite radius (r) as a function of time (t). At a fixed crystallization temperature, the plot of (r) vs. (t) is linear and its slope gives the value of G:

$$G = \frac{dr}{dt} \tag{2}$$

The influence of the Fe_3O_4 nanoparticles on the rate of radial growth (G) of iPP is illustrated in Figure 6. According to the figure, G values decrease with increasing crystallization temperature. In general, for melt crystallization, higher temperatures can result in the decrease of the degree of supercooling and consequently the decrease of growth rate.[18]

Conversely, no significant effect of Fe_3O_4 nanoparticles on the growth rate of iPP crystal can be noticed at each crystallization temperature. Thus it becomes clear that the reason of enhancement of overall crystallization rate is due to the presence of nano Fe_3O_4 as a nucleation agent, and has nothing to do with the spherulite growth rate. Ning et al. demonstrated that these results indicate that the nucleation and growth of a spherulite are two independent processes for the composites.[19]

Nonisothermal crystallization can be used as an alternative method to determine the spherulite growth rates, in which crystallization is monitored during cooling at a constant rate. This method permits, with a single experiment, to gain data in a

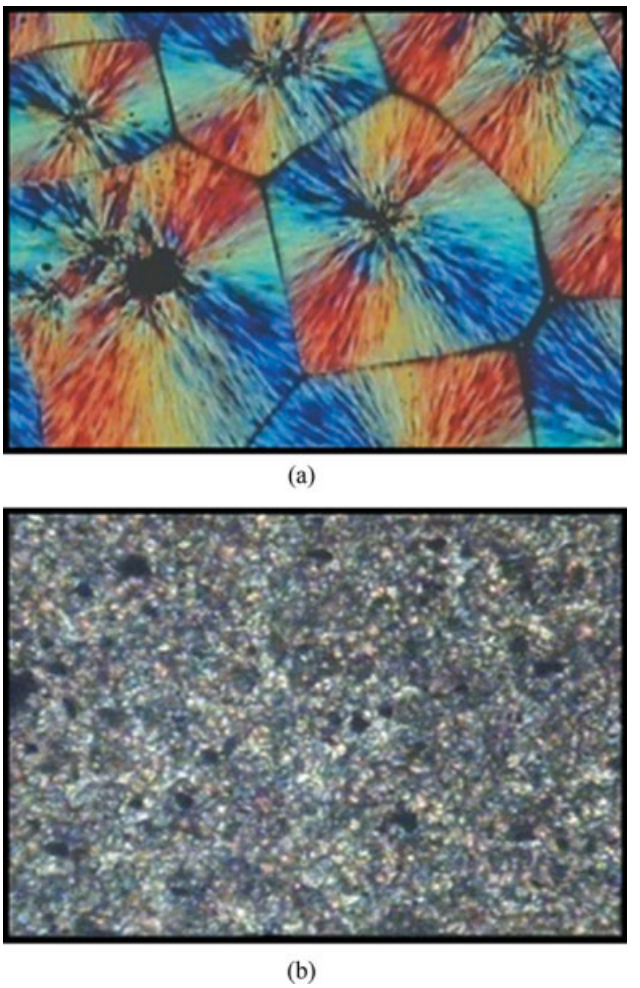

Figure 3 (a) iPP (b) 2% iPP/Fe_3O_4 nanocomposite samples crystallized at temperature 135°C. [Color figure can be viewed in the online issue, which is available at www.interscience.wiley.com.]

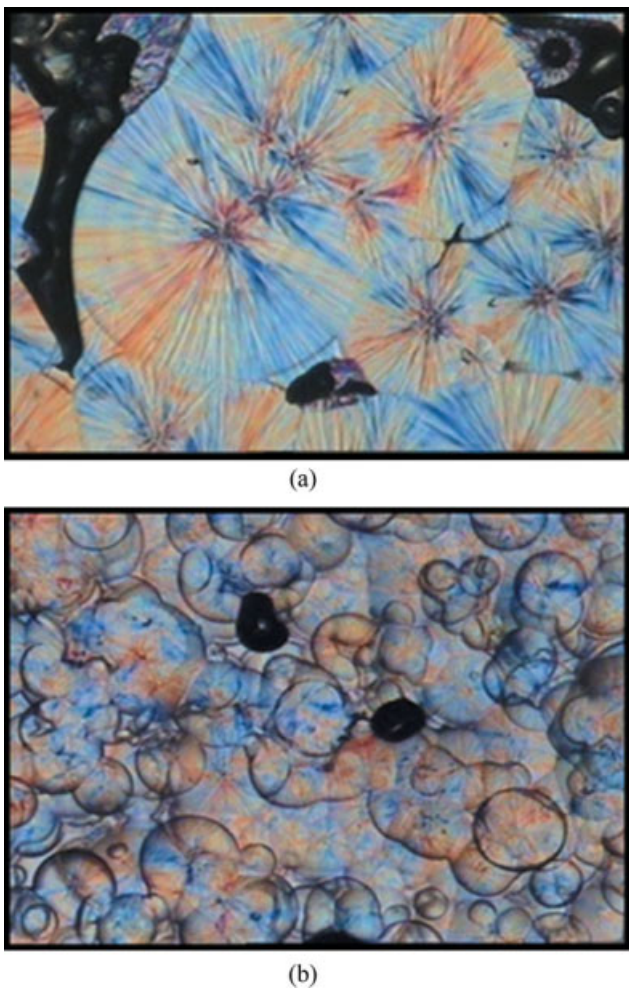

Figure 4 iPP spherulites crystallized at cooling rate, (a) 1°C/min; (b) 20°C/min. [Color figure can be viewed in the online issue, which is available at www.interscience.wiley.com.]

rather wide temperature range compared with the isothermal crystallization.[20,21]

Figure 7(a,b) shows a typical example for the nonisothermal spherulite growth for pure iPP and 2 wt % iPP/Fe_3O_4 nanocomposites at cooling rates of 1, 2, 5, 10, and 20°C/min. The nonisothermal spherulite growth shows a nonlinear behavior due to the change in temperature during the crystallization. Also it can be noticed that at a high cooling rate, spherulites approximately grow linearly. Spherulite growth rate, G was estimated by taking the first derivative of the spherulite radius vs. time curve at different times.

A Table Curve 2D software version 5.01, was used to calculate the G values. The G vs. T plots for pure iPP and 2 wt % iPP/Fe_3O_4 nanocomposite at different cooling rates are shown in Figure 8(a,b). From the figure it can be noticed that high cooling rates permit obtaining G values at lower temperatures compared with the isothermal crystallization since G

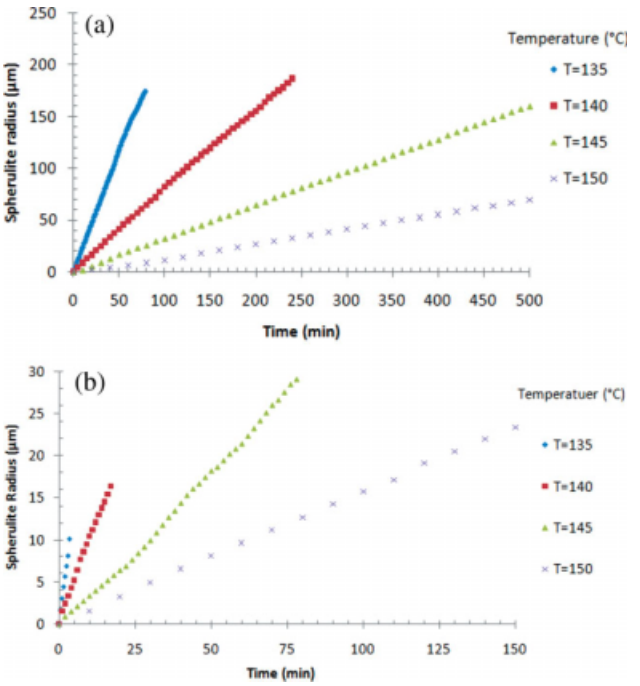

Figure 5 Spherulite radius versus time curves at different crystallization temperatures: (a) for iPP (b) for iPP with 2% nano Fe_3O_4. [Color figure can be viewed in the online issue, which is available at www.interscience.wiley.com.]

values can be hardly measured at low temperatures because of the high nucleation and growth rate. With nonisothermal method, instead, data can be measured at rather lower temperaures. It is also noticed that for pure iPP samples, Figure 8(a), the growth rate curves are almost overlap for low cooling rates 1, 2, and 5°C/min, (i.e. temperatures above 120°C) while the curves are scattered for high cooling rates, 10 and 20°C/min, (i.e. below 120°C). This scattered behavior can be attributed to the homogeneous crystallization and growth of the spherulites in the absence of the nucleation efficiency.[21] On the

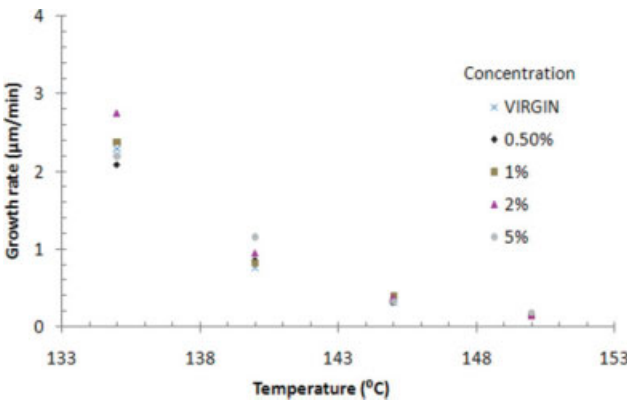

Figure 6 Growth rate of iPP with and without nano Fe_3O_4 as a function of crystallization temperature. [Color figure can be viewed in the online issue, which is available at www.interscience.wiley.com.]

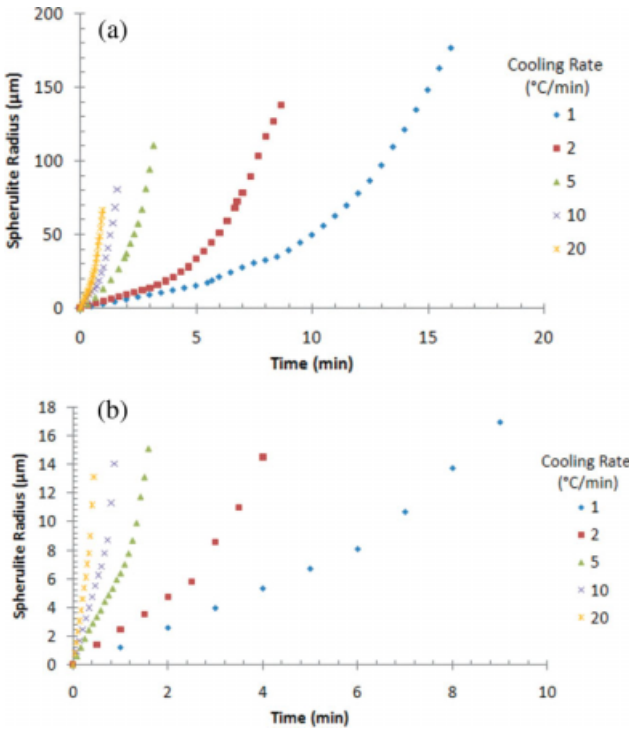

Figure 7 Spherulite radius of samples crystallized nonisothermally at different cooling rates as a function of time (a) iPP (b) 2% iPP/Fe_3O_4 nanocomposite. [Color figure can be viewed in the online issue, which is available at www.interscience.wiley.com.]

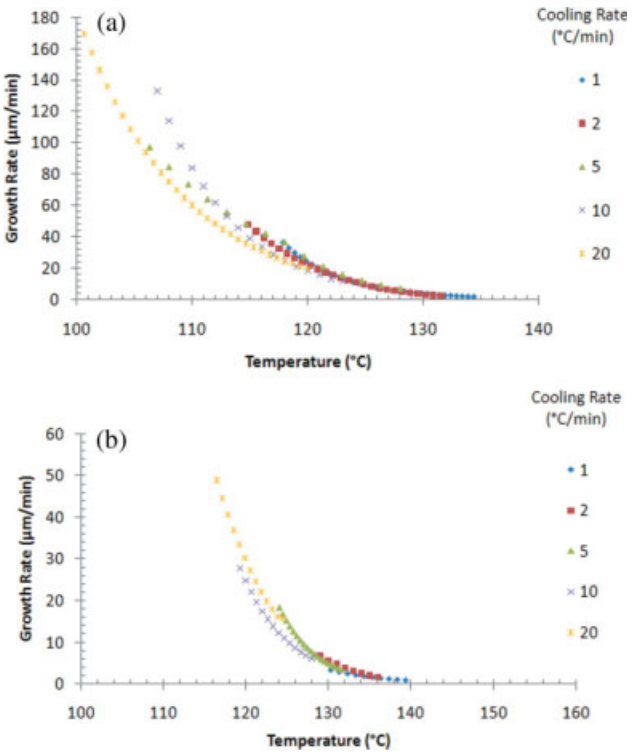

Figure 8 Growth rate of samples crystallized nonisothermally at different cooling rates (a) iPP (b) 2% iPP/Fe_3O_4 nanocomposite. [Color figure can be viewed in the online issue, which is available at www.interscience.wiley.com.]

other hand, Figure 8(b) shows almost overlap growth rate curves for the whole different cooling rates which proofs the effect of the Fe_3O_4 nanoparticles as a nucleating agent and this leeds to a heterogeneous crystallization process starts and completes at higher temperatures, also this means that cooling rate doesn't affect much the spherulite growth rates.

In Figure 9 the spherulite radial growth rate of pure iPP and iPP/Fe_3O_4 nanocomposites are reported for comparison. At each cooling rate, *G* values for all samples at a given temperature is almost the same. This is in agreement with measurments performed in isothermal conditions, and attributed to the enhancement of overall crystallization rate due to the presence of nano Fe_3O_4 as a nucleation agent, and has nothing to do with the spherulite growth rate.

A comparison between the isothermal and nonisothermal growth rates for the virgin iPP and 2 wt % iPP/Fe_3O_4 nanocomposite samples is presented in Figure 10(a,b). The growth rates data obtained with isothermal and nonisothermal methods are in a good agreement at cooling rate 1°C/min. These results are similar to the results obtained by,[5] where *G* values for un-nucleated iPP were the same at cooling rate 1°C/min. This is expected because at this slow cooling rate the range of temperatures at which the crystallization process started and completed falls within the covered range of the isothermal crystallization covered in the present work (135– 150°C). The agreement of spherulite growth rates obtained with isothermal and nonisothermal crystallization at cooling rate 1°C/min proves that the use of a nonconstant temperature during measurements doesn't affect the experimental determination of *G*.[21] At other cooling rates of 2, 5, 10, and 20°C/min, crystallization started at lower temperatures out of the isothermal range covered in the present work; hence, the growth rates at these cooling rates cannot be compared with the isothermal growth rates.

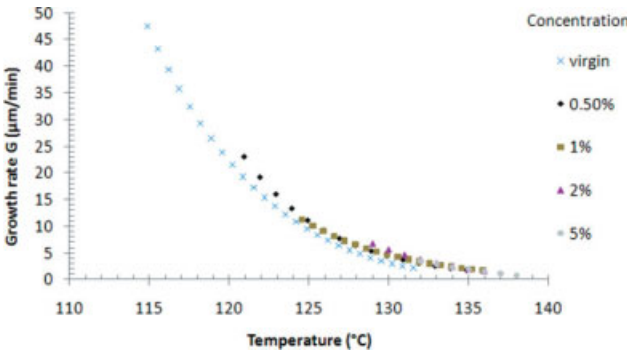

Figure 9 Growth rates of iPP with and without nano Fe_3O_4 nonisothermally crystallized at cooling rate of 2°C/min. [Color figure can be viewed in the online issue, which is available at www.interscience.wiley.com.]

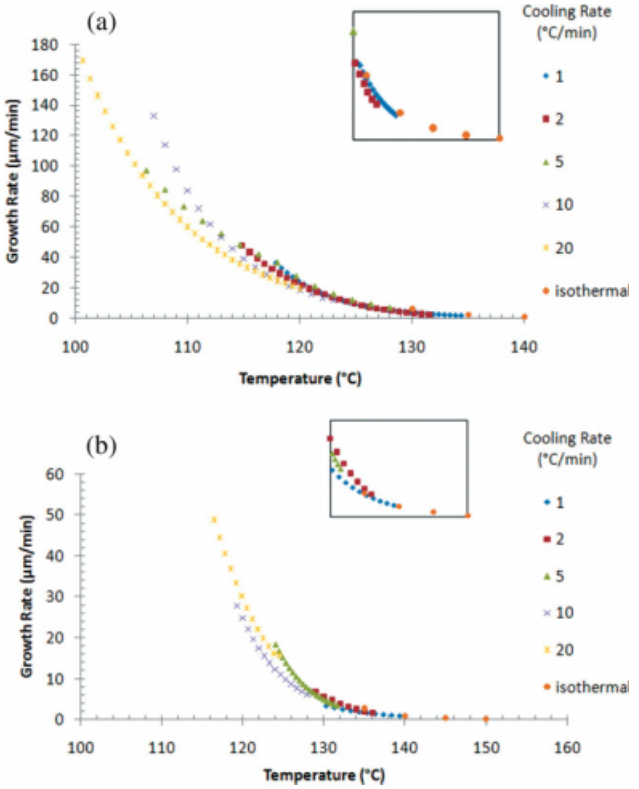

Figure 10 Comparison between isothermal and nonisothermal growth rate of (a) iPP (b) 2% iPP/Fe_3O_4 nanocomposite. [Color figure can be viewed in the online issue, which is available at www.interscience.wiley.com.]

Effect of Fe_3O_4 nanoparticles on the thermal properties of iPP

Figure 11 shows the second melting scan of DSC for iPP crystallized at different cooling rates. According to the figure and Table I, only one fusion endothem is present at cooling rates 1 and 2°C/min. While double fusion endotherms are presented at faster cooling rates of 5, 10, and 20°C/min. Numerous studies have shown that the type of both endotherms crystallize with monoclinic α crystal structure.[5,22–24] The locations of the peaks shift to lower temperature upon increasing cooling rate. This indicates that smaller size or less perfect crystals are formed under fast cooling conditions, since less time is available for crystallization during cooling. Rye et al. indicated that the effect of cooling rates on disappearance of the double peaks shape during heating is related to the degree of recrystallization or reorganization which becomes more significant for the lower molecular weight sample.[24] Yadav and Jain attributed the appearance of such double endotherms to several factors such as two different crystal forms, discrete bunching of crystallites of varying degrees of perfection, difference in crystals size, etc.[23] On another note, Figure 13 shows a trace of a very weak melting peak at ~ 147°C for the cooling rates 1, 2, and 5°C/min. This indicates that the sample contains small portions of β form crystals. The melting temperature of the β forms was observed to be around 145–150°C.[3,24]

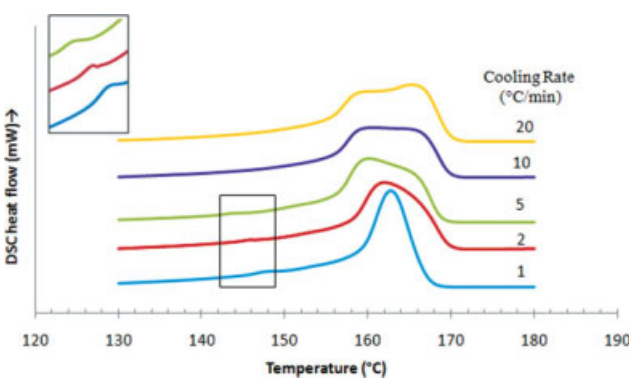

Figure 11 DSC melting curves for iPP crystallized at different cooling rates. [Color figure can be viewed in the online issue, which is available at www.interscience.wiley.com.]

TABLE I
Melting Temperatures of Nonisothermally Crystallized iPP Samples

Cooling rate (°C/min)	β-Spherulite melting temperature (°C)	α_1-Spherulite melting temperature (°C)	α_2-Spherulite melting temperature (°C)
1	146.5	162.6	–
2	145.5	162.0	–
5	144.3	160.16	165.5
10	–	159.6	166.1
20	–	158.5	166.29

Figure 12(a–e) shows the endothermic curves of DSC melting runs of pure iPP and iPP/Fe_3O_4 nanocomposites prepared by the masterbatch technique that were nonisothermally crystallized at cooling rates of 1, 2, 5, 10, and 20°C/min. It can be observed that the melting temperature T_m is shifting to a higher temperature upon increasing the nano Fe_3O_4 concentration. An increase from ~ 160 to 166°C is observed for all curves which indicates the heterogeneous nucleation effect of the nano Fe_3O_4 (Table II).

At cooling rates of 1, 2, and 5°C/min, small portions of β crystals appeared beside α crystals for the pure iPP and this is expected because at these cooling rates the onset temperature of crystallization starts at high temperature (130°C for cooling rate of 1°C/min to 126°C for cooling rate of 5°C/min), this range of temperature is in favor for β crystals to grow within.[5] Jacoby also found that in the temperature range 126–138°C, β-crystals grow faster than α-crystals.[25] At high cooling rates, 10 and 20°C/min, the onset temperature of crystallization falls bellow 125°C which does not allow the β crystals to grow.

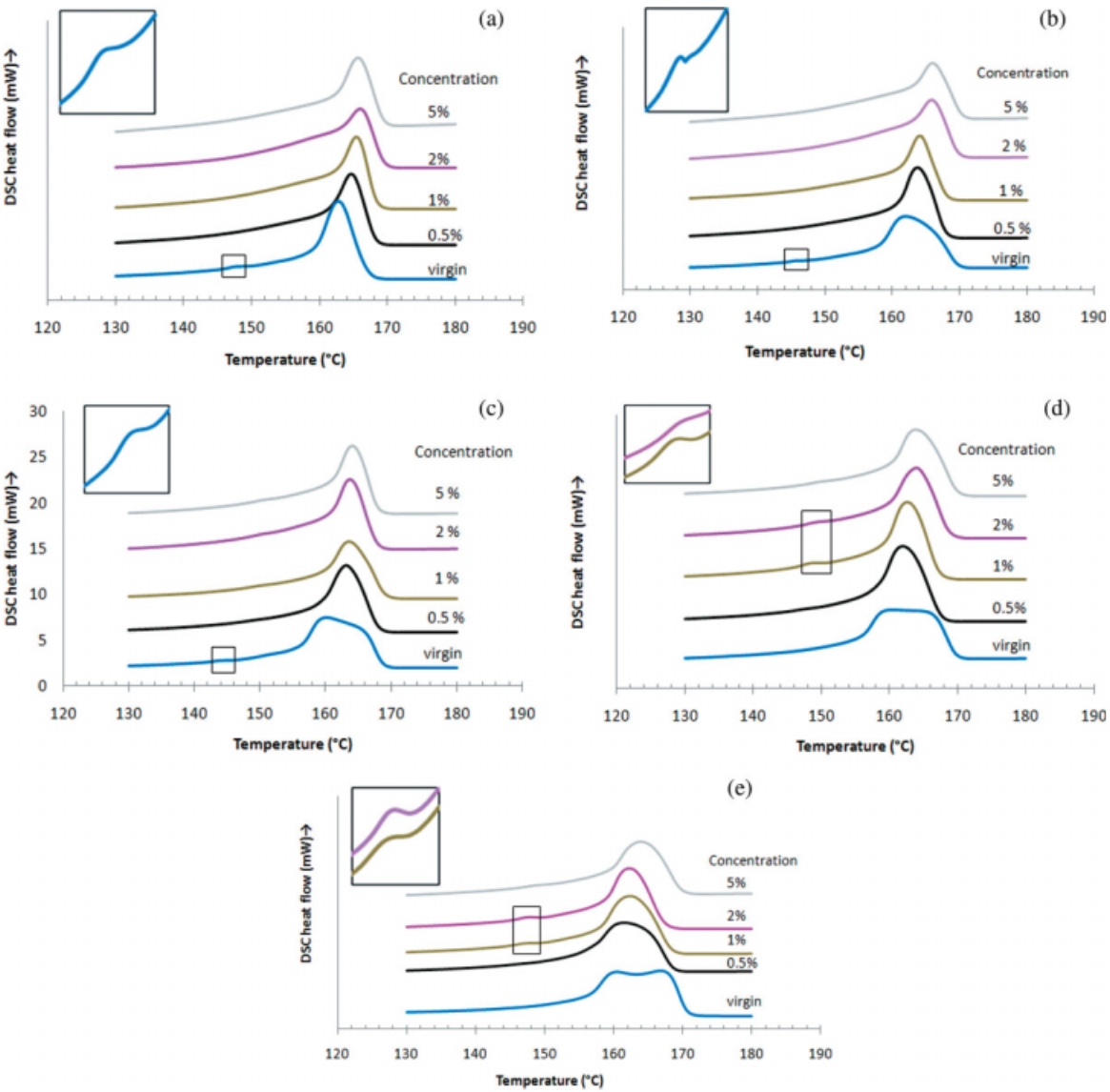

Figure 12 DSC melting curves for pure iPP and iPP/Fe_3O_4 nanocomposites crystallized nonisothermally at cooling rate (a) 1 (b) 2 (c) 5 (d) 10 (e) 20°C/min. [Color figure can be viewed in the online issue, which is available at www.interscience.wiley.com.]

On the other hand β and α crystals appeared only for the 1% and 2% iPP/Fe_3O_4 nanocomposites crystallized at high cooling rates, 10 and 20°C/min, this is again can be attributed to the onset temperature of crystallization. Increasing the percentage of the Fe_3O_4 nanoparticles will increase both the nucleation efficiency and the onset temperature of crystallization, the range of temperature that is in favor for β

TABLE II
Melting Temperatures of iPP and iPP/nano Fe_3O_4 Composites Crystallized at Cooling Rates 1, 2, 5, 10, and 20°C/min

Fe_3O_4 Concentration %	Cooling rate 1°C/min	Cooling rate 2°C/min	Cooling rate 5°C/min	Cooling rate 10°C/min	Cooling rate 20°C/min
0.0	162.6	162.0	160.1	159.6	158.2
0.5	164.6	163.6	163.1	162.0	161.5
1	165.3	164.0	163.5	162.7	162.33
2	166.0	165.8	163.6	164.0	163.5
5	165.8	166.0	164.1	165.7	165.2

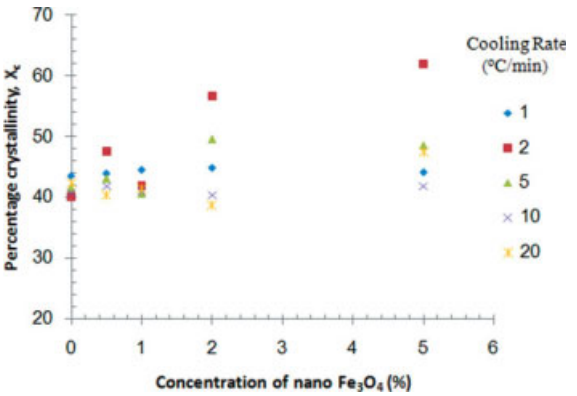

Figure 13 Percentage Crystallinity of iPP and iPP/nano Fe_3O_4 composites crystallized at cooling rates 1, 2, 5, 10, and 20°C/min. [Color figure can be viewed in the online issue, which is available at www.interscience.wiley.com.]

crystals to grow within occurs only for the sample containing 1 and 2 wt % of the Fe_3O_4 nanoparticles and cooled in the range between 10 and 20°C/min.

Also it seems that there is an optimum percentage of the Fe_3O_4 nanoparticles that can be added to iPP to encourage the formation of β-crystals and if this percentage is exceeded then the large amount of the Fe_3O_4 nanoparticles added will inhibit the formation of β crystals, we think this requires further investigation.

Figure 13 shows the percentage crystallinities, X_c, of pure iPP and the iPP/Fe_3O_4 nanocomposites samples crystallized at different cooling rates. In general, the figure reveals slight increase in the percentage crystallinity of iPP nanocomposites as the percentage of Fe_3O_4 nanoparticles increases. However, no uniform trends can be noticed for the percentage crystallinity especially at higher cooling rates. The presented results here are consistent with those in Ref. 26. This behavior of non uniform trend can be attributed to the fact that the addition of the nano Fe_3O_4 particles could have two types of effects on crystallization behaviors of iPP in iPP/Fe_3O_4 nanocomposites. On one hand, nano Fe_3O_4 particles may function as heterogeneous nucleating agents for iPP crystallization; on the other hand, nano Fe_3O_4 particles may hinder mobility and diffusion of iPP chains in the undercooled melt for crystallization. Decreases in mobility and diffusion of iPP chains can decreases the radial growth rates of iPP spherulites with increasing the nano Fe_3O_4 concentration.

Also as said before it seems that there is an optimum percentage of the Fe_3O_4 nanoparticles that can be added to iPP otherwise agglomeration will take place and reduce the percentage crystallinity and this should be investigated deeply.

Figure 14 shows the effect of cooling rate on the nonisothermal crystallization of iPP from the melt. It can be seen that the crystallization peak shifts towards lower temperature with increasing cooling rates, which means that the supercooling degree increases while the peak temperature, T_p, decreases. Also the crystallization peaks at low cooling rates are narrower than those at high cooling rates. When

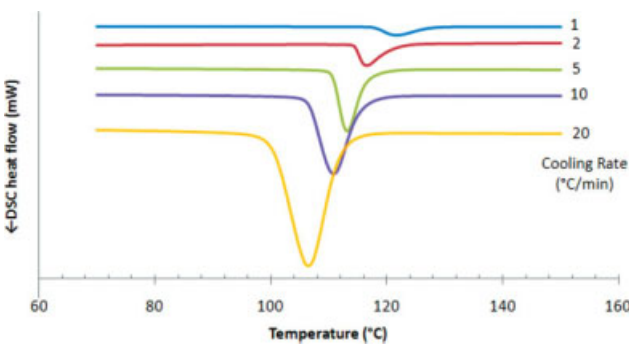

Figure 14 Nonisothermal exothermic curves of DSC at different cooling rates for iPP. [Color figure can be viewed in the online issue, which is available at www.interscience.wiley.com.]

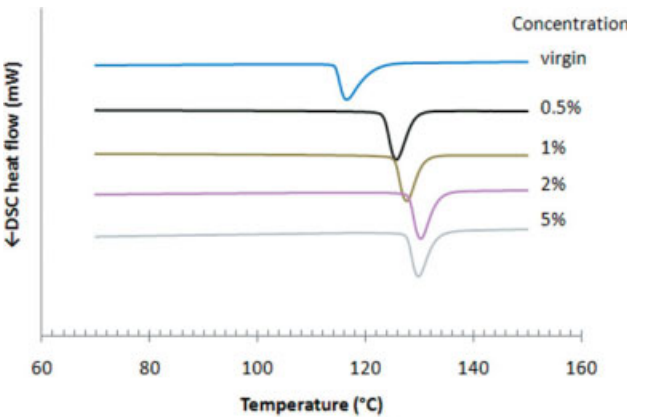

Figure 15 Nonisothermal exothermic curves for pure iPP and iPP/Fe_3O_4 nanocomposite at 2°C/min. [Color figure can be viewed in the online issue, which is available at www.interscience.wiley.com.]

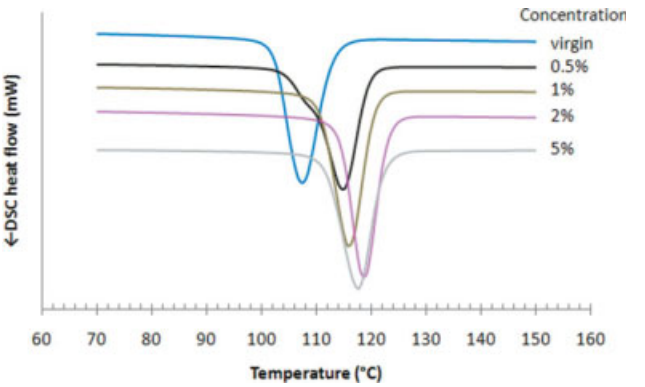

Figure 16 Nonisothermal exothermic curves for pure iPP and iPP/Fe_3O_4 nanocomposite at 20°C/min. [Color figure can be viewed in the online issue, which is available at www.interscience.wiley.com.]

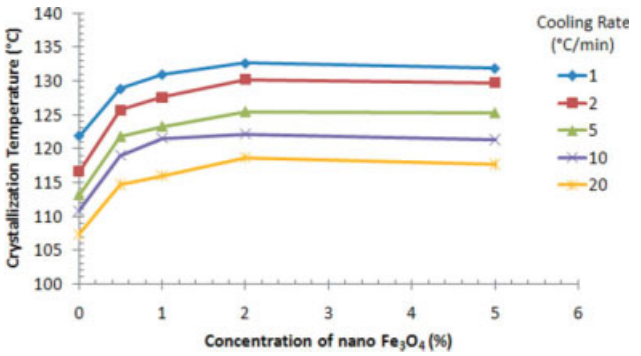

Figure 17 Effect of nano Fe_3O_4 concentration on the crystallization temperature of iPP at different cooling rates. [Color figure can be viewed in the online issue, which is available at www.interscience.wiley.com.]

the specimens are cooled fast, the mobility of the iPP chains is slow and hence they will not be able to follow the cooling temperature, thus retarding the crystallization[16] and so results in smaller size and less perfect crystals.[5]

Figures 15 and 16 are typical examples that show the crystallization curves of pure iPP and iPP/Fe_3O_4 nanocomposites prepared by masterbatch technique at cooling rate of 2°C/min. It is clear that at a given cooling rate, the crystallization peak temperature of iPP/Fe_3O_4 nanocomposites shifts to a higher temperature in comparison with pure iPP.

Also, the crystallization peak temperature is increasing upon increasing Fe_3O_4 nanoparticles content from 0.5 to 5%, The maximum shift in the crystallization peak temperature is about 20 to 21°C at the cooling rates of 1, 2, 5, 10, and 20°C/min as shown in Figure 17. This indicates the enhancement of dispersion process of the Fe_3O_4 nanoparticles in the iPP matrix upon using the masterbatch technique. It is obvious that the 2% masterbatch sample has the highest shift in the crystallization temperature. The lower shift of the crystallization temperature for the 5% masterbatch compared to the 2% masterbatch relates to the poor dispersion of the Fe_3O_4 nanoparticle, which indicates that the dispersion of the Fe_3O_4 nanoparticles is limited and Fe_3O_4 aggregation may take place at high concentration.[27]

CONCLUSIONS

1. Hyperbolic or straight-line boundaries between adjacent iPP spherulites can be obtained, which are mainly affected by the growth rate of spherulites. Usually, when the spherulites are nucleated simultaneously, straight lines boundaries are observed, while hyperbolic boundaries are observed when spherulites nucleate at different times.
2. Linear growth rates for isothermal crystallization were obtained, while nonlinear growth rates were obtained for iPP and iPP/Fe_3O_4 nanocomposite samples crystallized nonisothermally at different cooling rates as a result of temperature changes during crystallization.
3. No significant effect of Fe_3O_4 nanoparticles on the growth of iPP crystals is noticed. Thus it becomes clear that the reason of enhancement of the overall crystallization rate is due to the presence of Fe_3O_4 nanoparticles as a nucleating agent, and has nothing to do with the spherulites growth rate.
4. Fe_3O_4 nanoparticles act as efficient nucleating agent for isotactic PP. The presence of Fe_3O_4 nanoparticles in the iPP matrix inhibits the formation of β crystals and lead to higher shift in the melting temperature and an increase in the crystallization temperature upon increasing the Fe_3O_4 nanoparticles concentration in the iPP nanocomposite.
5. iPP/Fe_3O_4 nanocomposites prepared by the masterbatch technique indicate the enhancement of dispersion process of the Fe_3O_4 nanoparticles within the iPP matrix, which leads to less agglomerates in the iPP matrix, reduction of spherulite size and so produce higher effects on the crystallization behavior.

References

1. Grabiec, D. The development of a novel propylene nucleating agent, M.Sc. thesis, University of Massachusetts Lowell, 2003.
2. Mubarak, Y.; Martin, P. J.; Harkin-Jones, E. Plast Rubber Compos 2000, 29, 307.
3. Chen, X. Study on crystallization of isotactic polypropylene: effect of stereotacticity defects and nanofillers, Ph.D. thesis, Rensselear Polytechnic Institute-Troy, 2007.
4. Xu, W. Mechanical behavior, texture evolution and constitutive modeling of α and β crystalline isotactic polypropylene, Ph.D. thesis, The University of Michigan, 2003.
5. Mubarak, Y. A. A study of the crystallization and ageing of isotactic polypropylene, Ph.D. thesis, Queen's University of Belfast, 2000.
6. Treece, M. Processing, rheology, and crystallization dynamics of polypropylene-clay nanocomposites, Ph.D. thesis, University of Virginia, 2008.
7. Mai, Y.; Yu, Z., Eds. Polymer Nanocomposites; Woodhead Publishing Limited: UK, 2006.
8. Avella, M.; Cosco, S.; Leorenzo, M.; Pace, E. D.; Errico, M. E.; Gentile, G. Eur Polym J 2006, 42, 1548.
9. Chang, T. Microscopic mechanism reinforcement and conductivity in polymer nanocomposite materials, Ph.D. thesis, University of Akron, 2007.
10. Advani, S. G. Processing and Properties of Nanocomposites; World Scientific Publishing Co. Ltd: New York, 2007.
11. Jayaraman, K.; Kumar, S. Polymer Nanocomposites; Mai, Y., Yu, Z., Eds. Woodhead Publishing Limited: UK, 2006; 134.
12. Kruenate, J.; Tongpool, R.; Panyathanmaporn, T.; Kongrat, P. Surf Interface Anal 2004, 36, 1044.
13. Busch, D.; Hade, P.; Schmitz, B. U.S. Pat. 6, 992, 128 (2006).

14. Mishra, S.; Mukerji, A. Appl Polym Sci 2007, 103, 670.
15. Jain, S.; Goossens, H.; Van Duin, M.; Lemstra, P. Polymer 2005, 46, 8805.
16. Wang, D.; Gao, J. Int J Polym Mater 2004, 53, 1085.
17. Nisman, R. Morphological characterization of lamellar structures of single crystals and spherulites using atomic force microscopy and lateral force microscopy, M.Sc. thesis, University of Toronto, 1994.
18. Shangguan, Y.; Song, Y.; Zheng, Q. Polymer 2007, 48, 4567.
19. Ning, N.; Yin, Q.; Luo, F.; Zhang, Q.; Du, R.; Fu, Q. Polymer 2007, 48, 7374.
20. Di Lorenzo, M. L.; Cimmino, S.; Silvesto, C. Macromolecules 2000, 33, 3828.
21. Di Lorenzo, M. L.; Silvestre, C. Thermochim Acta 2003, 396, 67.
22. Norton, D. R.; Keller, A. Polymer 1985, 26, 704.
23. Yadav, Y. S.; Jain, P. C. Polymer 1985, 27, 721.
24. Rye, S. H.; Gogos, C. G.; Xanthos, M. Polymer 1991, 32, 2449.
25. Jacoby, P.; Bersted, B. H.; Kissel, W. J.; Smith, C. E. J Polym Sci: Part B: Polym Phys 1986, 24, 461.
26. Xu, D.; Wang, Z. Polymer 2008, 49, 330.
27. Perrin-Sarazin, F.; Ton-That, M. T.; Bureau, M. N.; Denault, J. Polymer 2005, 46, 11624.